EXPERIMENTAL INVESTIGATION INTO THE EFFECTS OF REDUCED VERTICAL CENTRE OF GRAVITY OF AN ARTICULATED CONCRETE MATTRESS IN CURRENT FLOW

(DOI No: 10.3940/rina.ijme.2017.a3.433)

A Neville, **R McLaren**, **J Weber**, **C Chin**, **J Binns**, and **A Taylor,** Australian Maritime College, Australia

SUMMARY

An articulated concrete mattress model has been utilised to investigate the effects of reduced vertical centre of gravity on the stability of a 400 series block. Experimental testing was conducted at the AMC CWC, Beauty Point. To determine the effects that a reduced centre of gravity has on stability, the 3 by 3 articulated concrete mattress model was subject to pure uniform current flow. The subsequent forces were analysed with a six degree of freedom underwater force sensor. In order to gain a range of real world scenarios, the experimental model was tested at six flow angles ranging from -15 degrees through to 60 degrees, at 15 degree increments. Additionally, five fluid velocities starting at 0.6 m/s through to 1.4 m/s, at 0.2 m/s increments were investigated. These results explain how the inversion of a 400 series block increases its hydrodynamic coefficients and subsequently decreases its stability performance in current flow. Ultimately, this study provides experimental information for the installation of 400 series articulated concrete mattresses in the inverted orientation.

NOMENCLATURE

Symbol	Definition (unit)
A	Area (m^2)
A_D	Drag area (m^2)
A_L	Lift area (m^2)
ACM	Articulated Concrete Mattress
AMC	Australian Maritime College
C	Force Coefficient
C_D	Drag Coefficient
C_{INT}	Confidence interval (%)
C_L	Lift Coefficient
C_{OVT}	overturning moment coefficient
CWC	Circulating Water Channel
F	Force (N)
F_D	Drag force (N)
F_L	Lift force (N)
g	Acceleration due to gravity (m/s^2)
H_{MP}	Height to pivot point (m)
M_{OVT}	overturning moment (N m)
n	number in the sample
s	standard deviation of the sample
t	confidence interval of the distribution
v	velocity (m/s)
V_{ACM}	ACM volume (m^3)
$v_{F,A}$	Failure velocity at A (m/s)
$v_{F,B}$	Failure velocity at B (m/s)
W_S	Submerged Weight (N)
ρ	density (kg/m^3)

1. INTRODUCTION

The implementation of manufactured and naturally formed marine structures in rivers and oceans has led to the issue of scouring, which occurs where the structure meets natural or unnatural fluid flow. In the case of a structure meeting fluid flow, its presence can alter the field of flow around its immediate environment. Scouring occurs as induced vortices around the structure remove seabeds, sand and mud (Young & Testik 2009). Pipelines are susceptible to scouring and can fail due to the removal of sand or sediment along the length of the pipe. This is a common issue in industry as pipelines can fail at the scoured location, due to bending under self-weight and contents. There are many ways to mitigate the destruction that scouring creates. Riprap, is a common countermeasure on bridge abutments and embankments to prevent scour, but possess negative traits as it is subject to dislodgment and slump; as well as slide failures (Melville 2006). Due to the economic cost of this method of pipeline protection and associated problems, new methods of technologically advanced protection have been developed.

Articulated concrete mattresses (ACM) are one such option that can provide stability throughout design life. An ACM is comprised of a series of individual concrete blocks placed to form a matrix revetment with specific hydraulic performance characteristics (Abt *et al*. 2001). They can provide a flexible alternative to riprap or rigid revetments; individual units are commonly held together by either steel rods, cables or rope. Typical failure modes of ACM's are the overturning and rollup of the edge exposed most to the flow, or the leading edge of the mattress. In addition, the uplift at the centre of the mattress is also a possible mode of failure. The uplift occurs when the leading edge is incorrectly anchored (Lagasse 2007). There is no industry standard stability design methodology to appropriately estimate the hydrodynamic forces of drag and lift (Godbold, Sackmann & Cheng 2014). Recommended practice outlines in situ conditions and requirements that need to be taken into consideration when calculating pipeline stability, in environmental conditions such as typical wave and current loads (Veritas 1988). The knowledge gap between predicted and encountered forces acting on an ACM still exists as recommended practices only contains design methods for dynamic lateral stability of pipelines. Recommended practice acknowledges that

ACMs are to be engineered to the correct shape, size, flexibility, density and ultimate strength (Veritas 2007). It is common industry practice to implement pipeline stability design equations and large safety factors that have the potential to over engineer ACM design. In the interest of improving the design procedure for ACMs, experimental and numerical research is necessary to determine non-dimensional hydrodynamic coefficients of drag and lift. In doing so, realistic estimations of these forces can be calculated that have the potential to reduce the cost of materials and labour in the build and installation process.

When an ACM is placed in protective environments such as pipeline protection, it will require specific minimum properties such as size, submerged mass, flexibility as well as overall concrete density. The stabilisation effects that an ACM possesses is generated by the submerged mass resting on the sea floor or object, as well as its geometric profile that can reduce overall drag and lift acting on the block itself. Companies such as Subcon produce three full ACM blocks that are 300, 400 and 500 mm high, as well as half ACMs that are 150 and 250 mm high. These are illustrated in Figure 1. Offshore stabilisation companies deploy these ACMs in situations specific to requirements of the environment; as economical and cost effective practices are of high importance to clients. Therefore, if a cheaper and lighter option is more viable, the company is able to compete for more business. Thus, to be less conservative in the design stage, research is required in the hydrodynamic properties of these ACMs so that large safety factors are not required.

Initial research investigated current forces on a 2 by 4, 300 series ACM in the Australian Maritime College (AMC) Circulating Water Channel (CWC) (Francis 2013). Typical lift coefficients for the mattress were much lower than predictions from literature and much lower than that recommended by industry practice (Veritas 2007). In addition, the coefficients were lower than that predicted in computational fluid dynamics (CFD) due to the effects of diminished lift and drag forces located in the critical region where high drag occurs (Francis 2013). Further numerical research (CFD) was also performed on a simplified 500 series model that investigated a 3 by 8 matrix at flow angles of 0 and 45 degrees at varied current velocities (Griggs 2014). Recent research has included the testing of these forces on all block types 300, 400 and 500, which investigated the overall performance on each of these types of ACM and their relevant implications in industry (Mclaren 2015). Final conclusions showed that the 400 series ACM outperformed the 500 series, ultimately leaving the 500 series a less viable solution if the stability of the block is the underlying requirement. However, the 500 series can be used if weight is the requirement (such implications are pipeline protection and support), whilst the 300 series may be used if low drag and lift forces are present on them due to their smaller geometry.

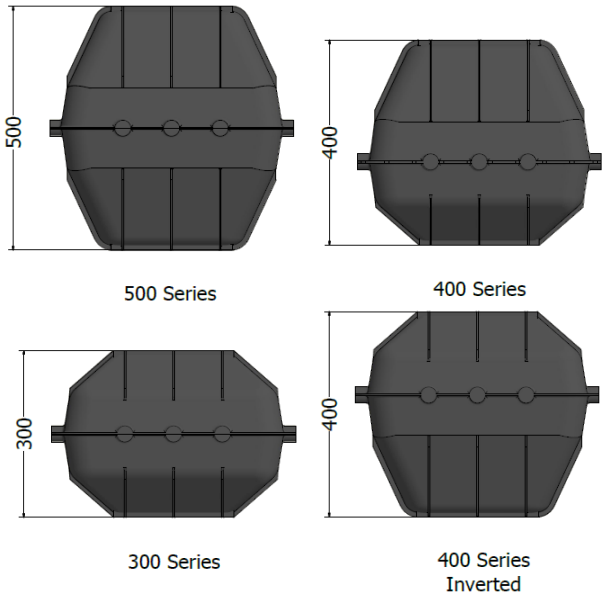

Figure 1: Summary of block types used for comparison in this paper

This paper will investigate how the stability of a 400 series ACM is affected by both the vertical shift upwards in the centre of gravity (COG) and a change in the centre of buoyancy (COB). The inverted 400 series will also be compared to other ACM sizes, to understand how it performs under the same experimental conditions, as well as investigating if it is a plausible option when compared with other block types. The increased COG position is to be achieved by inverting the geometry of a 400 series block. The inverted 400 series will be tested using the same model and procedure as Mclaren (2015).

2. THEORY

2.1 HYDROSTATIC AND HYDRODYNAMIC PROPERTIES

The COG of the submerged ACM block will be a contributing factor to the overall stability of the inverted 400 series block. It is assumed that the geometry of the block is consistent in shape, size and density; that is, it is a uniform object of mass. The centre of buoyancy of the object acts at the centre of the overall volume, which in this case, acts at the same position as the COG with the above condition. This is important for the calculation process as it is assumed the mass acts as point load through the COG, for simplification purposes in analysis.

2.2 FAILURE METHODS

A free body diagram of the forces acting on a submerged ACM is shown in Figure 2. Points A and B show the expected failure locations of an ACM in current flow. It is expected that in a matrix formation, the failure mode occurs at location A, due to the uplift of the most frontal block. Uplift occurs on the front row of the ACM, and causes the frontal blocks to flip over the second row

about point A. In this paper, failure is assumed and defined to be any movement off the datum. This definition is required as it is too difficult to quantify small uplifts that do not cause the front row of the ACM to fail.

Failure at point B is also taken into consideration due to the possibility that the ACM is disconnected or the joining articulation has failed. This failure method causes the ACM to rotate about point B, and turn over about this touch down position at the datum.

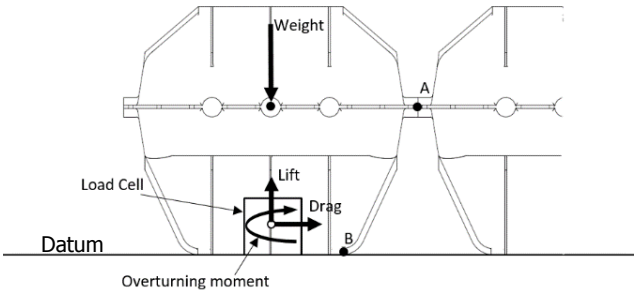

Figure 2: Summary of forces and failure locations (A and B) acting on an ACM due to failure methods

2.3 DRAG AND LIFT COEFFICIENTS

The non-dimensional coefficients of drag C_D and lift C_L can be used as a means of quantifying the hydrodynamic effects acting on an object. In this case, by rearrangement of the simplified Morrisons equation (Veritas 2010) shown in Equation (1), the coefficient can be calculated. Here F is force, ρ is the fluid density, A is projected area, v is the fluid velocity and C is a coefficient of the force.

$$F = \frac{1}{2}\rho A v^2 C \tag{1}$$

Equations (2) and (3) are used to evaluate the drag coefficient C_D and lift coefficient C_L (Veritas 2010). Here, ρ_{water} is density (in this case taken as 999.1 kg/m^3 (Mclaren 2015)), v is the water particle velocity, A_D is the drag area and A_L is lift area. The drag area of the block is taken as the frontal exposed area of the ACM block. In addition, the lift area is simply the top area of the ACM and the drag and lift areas are kept constant. The drag force F_D, and lift force F_L are the measured forces acting on the experimental load cell.

$$C_D = \frac{2F_D}{\rho_{water} A_D v^2} \tag{2}$$

$$C_L = \frac{2F_L}{\rho_{water} A_L v^2} \tag{3}$$

2.4 COEFFICIENT OF OVERTURNING MOMENT AND SUBSEQUENT FAILURE VELOCITY

A method of quantitatively measuring the stability is required and was proposed. A proposed overturning coefficient C_{OVT} is, in its most simple form, the combination of asymmetrical drag and lift about the centre of the load cell, or about the point acting as a hinge (Mclaren 2015). Due to the relationship of the overturning moment M_{OVT} to drag and lift, a simple area is not used. Thus, the volume of the object V_{ACM} is used for non-dimensionality, in this case, the volume of the ACM block. The formula for the overturning moment coefficient is given by Equation (4).

$$C_{OVT} = \frac{2M_{OVT}}{\rho V_{ACM} v^2} \tag{4}$$

The failure velocity is determined where the fluid creates an overturning moment equal to or greater than the submerged weight about the point of failure. This is determined by the summation of moments about the failure points A and B in Figure 2 and is defined as $v_{F,A}$ and $v_{F,B}$ respectively. Summation of moments includes drag force, lift force as well as the moment generated about the base of the ACM block. The summation of these forces give the failure velocities A and B and these are shown in Equations (5) and (6).

$$v_{F,B} = \sqrt{\frac{0.25W_{Submerged}}{\rho_{water}(C_{OVT}V_{ACM} + 0.038C_D A_D + 0.125C_L A_L)}} \tag{5}$$

$$v_{F,A} = \sqrt{\frac{0.50W_{Submerged}}{\rho_{water}(C_{OVT}V_{ACM} - (H_{MP} - 0.038)C_D A_D + 0.25C_L A_L)}} \tag{6}$$

Here, $W_{Submerged}$ is the submerged weight of an individual ACM block, other keys terms in Equations (5) and (6) have been defined in Equations (2) and (3), as they are kept consistent throughout this paper. The submerged weight of the ACM block is evaluated by the formula shown in Equation (7). It is important to note that H_{MP} is the height measured from the datum to the pivot point of the moment and is not simply half the height of the block in a 400 series. The numerical values for the failure velocity are simply a means of evaluating the performance of the block relative to one another. This will not be equal to the exact velocity at which a block will fail at in situ. Lastly, g is defined as the gravitational constant, $\rho_{concrete}$ is the density of concrete (taken as 2400 kg/m^3, as per McLaren (2015)) and V_{ACM} is the volume of the ACM block.

$$W_{Submerged} = gV_{ACM}(\rho_{concrete} - \rho_{water}) \tag{7}$$

The importance of these calculations is to determine and gauge the performance of each block type relative to each other. It is important to note environmental loads that the ACMs are exposed to in operation cannot be fully replicated in the CWC, and therefore do not accurately represent failure velocities expected whilst in operation. A better understanding of hydrodynamic coefficients of lift and drag will broaden industry knowledge and design processes. The research conducted in this paper will aid in mattress placement with respect to the type of ACM installed as well as its position with respect to the incident flow direction.

2.5 UNCERTAINTY ANALYSIS

In order to approximate the level of deviation in the experimental data, an uncertainty analysis is required. This can be achieved by evaluating the confidence interval at 97 % of the mean, of the non-dimensional coefficients at each velocity and angle. The sample confidence interval is determined using Equation (8) (Figliola & Beasley 2015), where s is the standard deviation of the sample, t is the confidence interval of the distribution and n is the number of samples in the source.

$$C_{Int} = t\frac{s}{\sqrt{n}} \qquad (8)$$

3. METHODS

The AMC CWC was used in the experimental investigation. The CWC is a large test facility that is 11m long, 5m wide and 2.5m deep that can produce water velocities up to 1.7 m/s (Australian Maritime College 2016). A glass window on the side of the tank allows for test viewing, as well as a means of inspection for problems or issues occurring during experiments.

3.1 EXPERIMENTAL CONFIGURATION AND PROCEDURE

The model scale used in the experimental testing of the inverted 400 series block was a full scale (1:1) Subcon concrete block mould. The mould consists of two half shells that are clipped together and fixed to a steel plate using threaded bar and a top plate. The top shell is a 150mm shell, and the bottom is a 250mm shell. The testing apparatus is an adaptation of that used by Mclaren (2015). It is important to note that the initial set up was fabricated by Francis (2013) and has been further modified for this experiment. The initial 2x4 mattress and plate has been improved to allow for a uniform 3 by 3 matrix shown in Figure 3. One block is constructed to mount the load cell for 6 degrees of freedom (Figure 4) within the block, whilst also simultaneously being secured to the steel plate. In addition, the block itself is positioned so that it does not interact with adjacent blocks.

The load cell was located in the centre block facing the flow, shown by the arrow in Figure 3. The load cell cable was tied down to the plate and surrounding blocks, and at the back to prevent movement and any possible interference from its vibrations in the fluid flow.

The load cell was located in the central block at the leading edge of the flow, as failure at the leading frontal block occurs first (Mclaren 2015). Thus, there was little reason to investigate the corner block of the matrix. The load cell was internally fitted within the centre block at the leading edge of the mattress, in order to measure forces when it was displaced. This requires the block itself to suspend off the steel plate and have the ability to move in all degrees of freedom. Lastly, it was imperative that the blocks did not touch and interfere with each other at any point, as this would induce forces previous experiments have not included or accounted for.

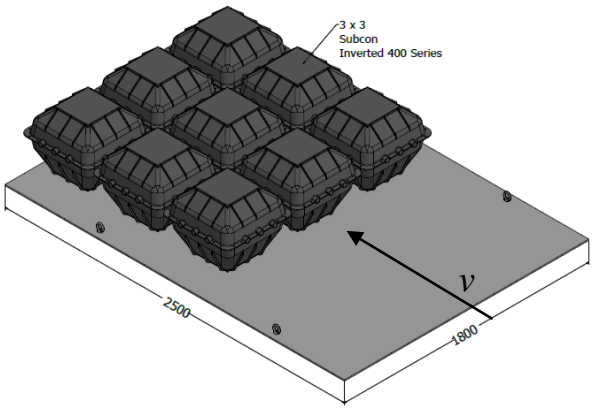

Figure 3: Experimental set up in mm, where the arrow indicates flow direction, *v*

This experiment was conducted such that the front row of the ACM was subjected to flow from the frontal side (load cell location). A summary of the testing regime for each angle of attack is shown in Table 1, where at the beginning of all angle runs, a zero value was recorded. The zero value takes into account all forces including hydrostatic pressure acting on the load cell at the bottom of the CWC. Testing procedure occurred such that two, 180 second readings of each pump velocity was recorded at each angle of attack. To reduce testing time, data was recorded whilst the water velocities were increased from the lowest to the largest and subsequently decreased in the reverse manner. Double readings were required to gain an average of the force over the testing duration.

Repeatability in the experiment is crucial in order to verify and cross check final data. The first set of repeatability checks conducted were the angles of attack. In the experiment, -15 and 15 degrees are theoretically the same angle assuming the model was positioned symmetrically in the CWC. The drag, lift and overturning moment coefficients were cross checked with the repeated 15 degree angle. The water velocity

within the tank was repeated after the maximum velocity was produced, with velocities of 0.8, 0.6 and 0 m/s. This action also aids in slowing down the velocity within the tank, in order to record another 0 m/s run.

Table 1: Testing regime at flow angles of attack -15, 0, 15, 30, 45 and 60 degrees

Run	Velocity(m/s)	RPM	Run	Velocity(m/s)	RPM
1	0	0	**8**	1.2	145
2	0.6	75.1	**9**	1.2	145
3	0.6	75.1	**10**	1.4	170
4	0.8	100.1	**11**	1.4	170
5	0.8	100.1	**12**	0.8	100.1
6	1	120.1	**13**	0.6	75.1
7	1	120.1	**14**	0	0

3.2 DATA ACQUISITION AND CALIBRATION

The underwater load cell was a six component force sensor with a stainless steel body that operates with an oil filled pressure compensation bladder to enable short term (less than 24 hours) immersion in fresh water (AMTI Force and Motion 2009). The six degrees of freedom load cell and calibration equipment are shown in Figure 4.

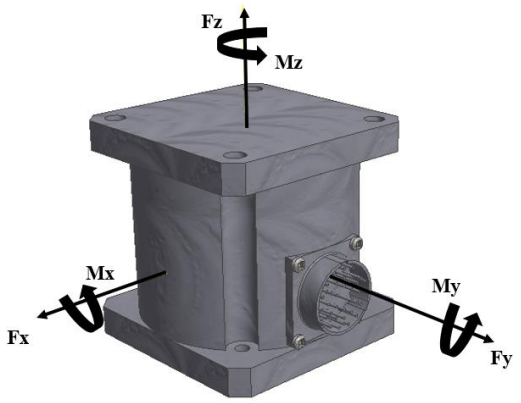

Figure 4: MC3-SSUDW underwater load cell used in the experimental procedure

Without a load cell calibration, the experiment would not be accurate or credible. Calibration is required to read accurate hydrodynamic forces whilst testing is in operation. The calibration technique involved taking registered readings of forces and moments in known directions including forces in Fx, Fy and Fz and moments in Mx, My and Mz. A relationship was generated by plot between the load applied and the output voltage. The relationship created is linear, and the resultant gradient is the calibration conversion from volts [V] to Newtons [N]. The voltage reading from the load cell can be converted to a force with the known calibration matrix K. Table 2 describes the calibration matrix used to process the raw data.

Table 2: Calibration matrix for the underwater load cell

Channel	1	2	3	4	5	6
	Fz	Fx	Mz	My	Mx	Fy
K [N/V]	30.045	7.793	0.211	0.146	0.140	8.135

4. RESULTS AND DISCUSSION

4.1 STABILITY

To gain an estimation of the change in the COG in a 400 series ACM block, its computer animated geometry was investigated. The COG can be measured from the datum or ground the block rests on. An increase in the COG leads to an overall reduction of the GM. As per Figure 5, the COG for an upright block is 203mm and the inverted block has a COG of 218mm. An overall change upwards of 15mm in the value of COG was measured.

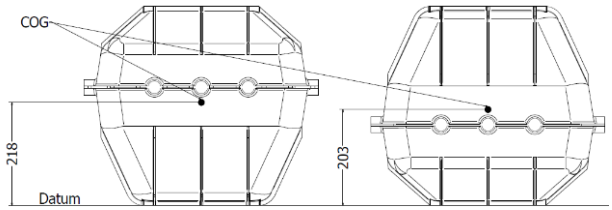

Figure 5: Location of COG (black circle) for; the inverted (left), and upright 400 series (right)

This 15mm shift upwards in COG translates to an overall increase of 6.88 %, measured from the datum. Although this is a relatively small variance in COG, the overall stability of the inverted 400 series is still expected to reduce. The likelihood of failure due to overturning increases when the COG shifts upwards from the datum. As the mass of the object acts through the COG, less overturning force is required to generate a moment greater than its submerged weight. This is due to a higher moment lever the 400 series ascertains after inversion, leading to increased instability.

4.2 BLOCK TYPE VALIDATION

Data collected from previous experimental analysis from Mclaren (2015) can be used to compare the performance of the inverted 400 series ACM. This data contains the same experimental methods of 300, 400 and 500 series.

4.3 DRAG AND LIFT COEFFICIENTS

Figure 6 and Figure 7 show the post processing results for the drag and lift coefficients respectively, using Equations (2) and (3). The repeatability angles of -15 and 15 degrees showed similar values of drag coefficient of 0.5 and lift coefficient of 0.3 as expected. The inverted 400 series shows the highest coefficient of drag at 0 degrees angle of attack and can be accounted for due to the large exposed frontal area of the block. As the drag coefficient is proportional to exposed frontal area, when

altering the angle, the drag force changes respectively, whilst the projected drag area remains consistent.

The study shows that the drag coefficient of the inverted 400 series is only higher than the upright 400 at this 0 degrees angle of attack. To verify the data, implementation of a 97% confidence interval in the load cell data was produced and shows little deviation from the mean result. Therefore, the drag coefficient determined in this paper is within an acceptable range, as the data does not deviate significantly from the mean. Uncertainty bars can be used to show this confidence interval and it is clear that varying degrees of overlap occur within the four sets of data as shown in Figure 6. It is also apparent that the difference between the 400 series and the inverted 400 is minimal, as significant overlapping occurs whilst increasing the angle of attack. For ease of analysis and clarity, Figure 6 is the only plot that indicates the uncertainty of the coefficients for simplicity and ease of analysis. It is assumed that other load cell channels used for the lift and overturning coefficients carry the same sample uncertainty. Therefore, the uncertainty bars illustrated in Figure 6 will not be present throughout the data plotted in this paper, due to congestion that prevent clear understanding of data points.

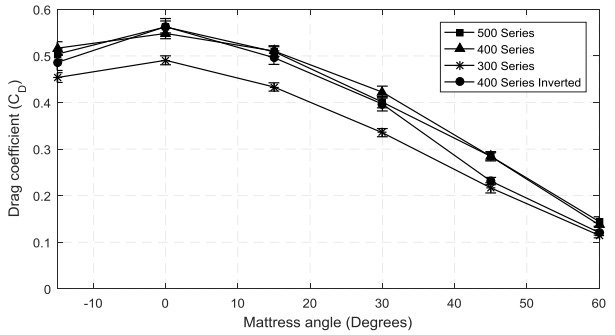

Figure 6: Drag coefficient comparison with 97 % confidence interval showing significant overlap between inverted 400 and upright 400 series, whilst the inverted 400 has higher drag at 0 degrees angle of attack

Overall, the change in drag force is not significant enough to simply imply the instability of the inverse 400 series. To quantify the instability, the lift force must also be examined, as this lift force significantly contributes to the failure mechanisms in conjunction with overturning moment.

The study shows that the lift coefficient of the inverted 400 series is higher than the upright 400 series in all angles of flow incidence. This is due to the geometry of the block, as it experiences higher differential pressure around the larger bottom area. The high pressure differentials in the xy plane (refer to Figure 4) acting between the bottom and top section of the block also causes this increased lift force. There is a significant difference in lift forces acting on the two 400 series shown in Figure 7. The difference in geometry between the two blocks causes large lift forces acting on the 250 mm section of the block and is mainly accounted for due to the large pressure on the face of the bottom shell as the velocity at the face reduces significantly. Figure 7 suggests decreased stability, resulting from a difference in lift coefficient of 0.1 that is clearly present between the upright and inverted 400 series. At angles of attack up to 30 degrees, this 0.1 differential in the trend is a common difference. It is clear that the inverted 400 series has similar lift forces when compared to the 500 series despite having considerably less weight. It is possible that the geometry of the 250 mm half shell induces these large lift forces. The impact of significantly larger lift forces in the lower 250 mm region causes the instability of the inverted 400 series to increase. High instability occurs due to more force that is able to lift the block off the datum. Another verification of reduced instability can be produced upon investigation of the moment (Mx) generated about the centre of the load cell. Although it is not a true representation of the failure moment force at the failure location, it gives a qualitative analysis between the upright and inverted 400 series.

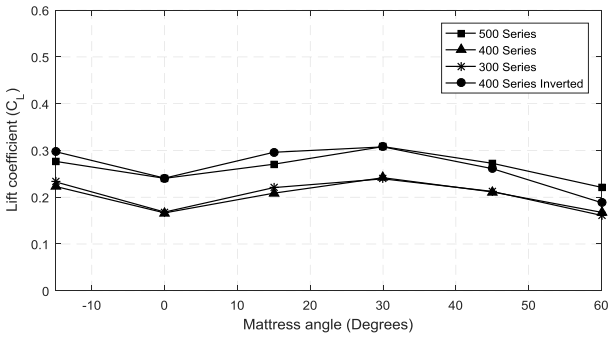

Figure 7: Lift coefficient comparison showing significantly higher lift for the inverted 400 series compared to the 400 series due to the 250mm bottom half section of the block

4.4 OVERTURNING AND FAILURE VELOCITY

The qualitative method of comparison mentioned in section 4.3 is the overturning moment coefficient. The overturning moment coefficient in the xz axis was calculated using Equation (4), and is plotted against the angle of attack shown in Figure 8. The overturning moment coefficient is a maximum at 0 degrees angle of attack. This is highest at this location due to large forces acting at this angle. It is evident that the inverted 400 series has higher moment coefficients at all angles of attack. Again, as the geometry of the 400 series suggests, a greater portion of the body resides at a higher location above the datum. Hence, the higher the force lever, the greater the moment for the same applied load. Higher moment forces suggest that the increased COG has an effect on the overall stability of the ACM. However, as the coefficient difference is only 0.08, the increase in COG has a lesser effect to the stability than originally hypothesised. It is important to note that the data presented in Figure 8 follows expected theory. The 500 series ACM has the highest overturning moment

coefficient as it is the largest block. Conversely, the 300 series has the least as it is the smallest block. The location of the overturning moment coefficients gives credibility to the location of the moment acting on the inverted 400 series, as the 400 series' data lies just below the 500 series, yet, above the upright 400 series.

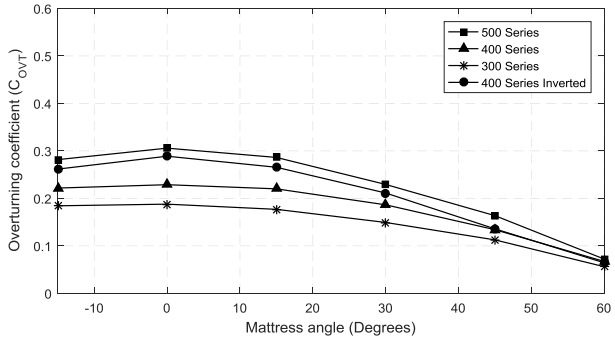

Figure 8: Overturning coefficients showing higher moment forces acting on the inverted 400 series

Failure flow rate is the fluid velocity required to cause enough hydrodynamic force of drag, lift and overturning moment that will result in the ACM failure at points A or B shown in Figure 2. For this reason, the failure velocity is a comprehensive way of comparing the stability of each ACM block size, as it takes into account the submerged mass of the block, as well as the lever arms to the connections. The failure velocity equation takes drag, lift and overturning moment about the location of failure, and solves for velocity.

The failure flow rate values are again plotted against the angle of attack. Figure 9 displays the velocities that will cause the block to fail at point A. The trend shows a similarity between the upright and inverted 400 orientations, in that they do not diverge significantly away from each other throughout the increment in angles of attack. The trend is due to the moment lever used in the failure velocity in Equation (6). The H_{MP} term, or the moment lever in Equation (6), is larger for the inverted 400 series, meaning that the overall velocity decreases as the moment is larger. The upright 400 series moment is smaller yet the failure velocity is larger, which causes the failure velocity to become closer together. Although the failure velocity at 0 degrees angle of attack is 5% higher than the upright orientation, this justifies the inverted orientations instability in current flow. Lastly, the failure flow rate at point A shows that when an ACM is deployed, it is imperative that it is positioned such that it is able to withstand current forces at the 30 degree angle, as this is the position at which it will fail first. The 30 degree angle of attack position experiences the greatest amount of force that will cause it to fail due to uplift of the most frontal block.

Failure at point A assumes that the ACM is connected by some degree of articulation, either by steel rods, wire, or rope; such that the connection is relatively rigid. This means that a block adjacent to another block at the leading edge has additional effects on the mass and stability of that at the front. However, this study does not take into account these effects.

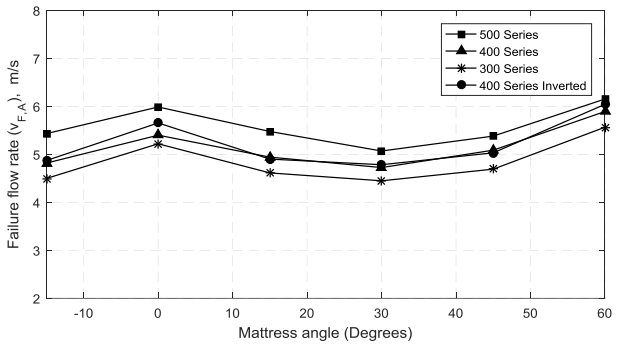

Figure 9: Failure flow rate for location A, illustrating the convergent nature of the inverted and upright 400 series comparison

Analysis of the failure flow rate at location B is also a way of quantifying the stability of the inverted 400 series ACM. Location B is located where the bottom of the ACM meets the datum, and so summation of moments are taken at this point and consequently no vertical moment lever arms are present, which is similar to the condition of failure flow rate at A. Having only horizontal moment arms and constant downward moment levers (between the load cell and the datum), the converging nature of failure at point A does not exist. Hence, an appropriate comparison was obtained, as the difference in inverted 400 and upright 400 is consistent, due to the nature of the block geometry.

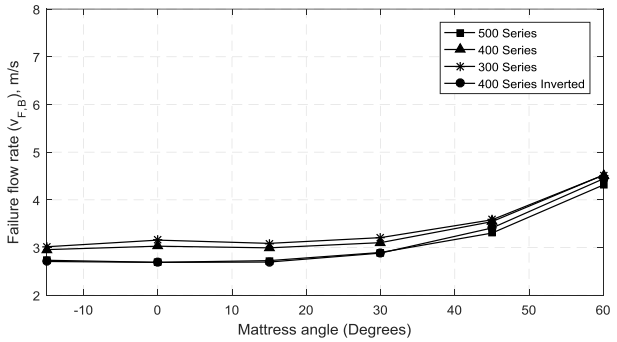

Figure 10: Failure flow rate for location B, displaying the small contrast in failure velocity of a maximum 0.3 m/s between the inverted and upright 400 series

An exponential trend is apparent in Figure 10, as the further the angle is away from the flow, the greater the force is required to cause the block to fail. More force is required at higher angles as the corner block physically blocks the centre face block. For that reason, the load cell is not exposed to large amounts of flow, and subsequent high failure velocities are present at 45 and 60 degrees. This plot is significant, as the inverted 400 series will fail at point B, 0.3 m/s before the upright position at the 0 degrees angle of attack. Notably, the failure velocity at point B stays relatively constant throughout the increase in angle of attack. This is a critical factor in offshore

applications when an ACM fails at position B. Failure at point B can occur if the joining articulation between blocks has failed, or is damaged. The phenomenon of relatively constant failure flow rate means that in scenarios where a block experiences flow angles over a 45 degree spread (0 to 45 degrees angle of attack) the block should experience similar forces about the failure location B. In addition, it is further confirmation that the vertical shift upwards in COG reduces the 400 series' stability. The shift in COG of 15mm upwards has not affected the overall stability of the inverted 400 series as much as initially predicted, according to the failure velocity at point B.

4.5 LIMITATIONS

Sources of uncertainty in this experiment may have originated from a range of experimental methods. Firstly, possible creep from the load cell can occur when it experiences load for an extended period of time. This is common for the load cell used in this experiment and it is possible that it has affected the results. The fluid profile at the CWC is another possible source of uncertainty, as the velocity the experimental set up experiences may not be the same as the input velocity. This issue can be overcome by regular flow profile checks throughout experimentation. This eventuates into uncertain hydrodynamic coefficients, as the values are calculated at incorrect velocities.

Sample uncertainties in this paper were analysed and an uncertainty confidence interval of 97 % was determined. The average range of this uncertainty was determined to be 0.011, which was a maximum of 7%, and a minimum of 2% of the data produced.

Lastly as the density of concrete assumed for this paper is 2400 kg/m^3, the failure velocity predicted is the worst case scenario. Thus, if the density is assumed to be higher (which can be up to 5000 kg/m^3 in industry applications) than this, the subsequent failure velocity will significantly increase, as the total force required to overturn the block and cause failure increases.

5. CONCLUSIONS

An experimental articulated concrete mattress set up in the AMC CWC has been successfully performed to determine stability effects of a 400 series Subcon block with a reduced centre of gravity. Reduction of the centre of gravity was achieved by inverting the ACM, and analysed by comparison of the hydrodynamic coefficients of drag, lift and overturning moment. A failure velocity in two locations was used to determine the overall effects of all combined forces, including submerged mass. It was anticipated that the inverted 400 series would show significantly less stability, due to the change in centre of gravity upon inversion. Upon inspection of computer animated geometry of the 400 series, the overall decrease in centre of gravity measured from the bottom of the block was 15 mm once the geometry was inverted, which was significantly less than first anticipated.

Analysis of the drag, lift and overturning moment coefficients concluded that the difference in lift coefficient is a maximum of 0.1, at 0 degrees angle of attack. This is consistent throughout the change in angle. Higher lift coefficient of the inverted 400 series was predictable due to the larger 250 mm section of the block at the bottom on the body. This instigated greater lifting forces acting on the bottom region and also translates into the coefficient of overturning that this lift force creates. The overturning coefficient is also 0.08 greater at 0 degrees angle of attack and is seen to decrease throughout the increase of angle of attack, as the mattress body and load cell block experiences less force, since it is less of a bluff body.

It is clear that the inverted 400 series displays lower stability than that of the upright orientation, as the inverted 400 series experiences considerably higher lift forces at all angles of attack, as well as slightly higher drag at 0 degrees angle of attack. In addition, the subsequent predicted failure velocity of the inverted 400 series is greatest at 0 degrees angle of attack and is 0.3 m/s higher compared to its correct orientation. The analysis shown in this paper illustrates that the use of the inverted 400 series has a reduced capability over the upright 400 series ACM block. If installation of the 400 series is to occur in industry, it would be eminent to the client that the blocks for the ACM should not be in the inverted position, if the failure velocity in this paper is to be considered in design calculation.

6. ACKNOWLEDGEMENTS

The author would like to extend his acknowledgements to the following people for their contributions to this experimental investigation. The supervisor Mr Josh Weber, the Co supervisor Mr Rory McLaren, A/Prof Jonathan Binns, Dr. Christopher Chin, Murphy McColl, Alex Taylor and Simon Little.

7. REFERENCES

1. ABT, S, LEECH, J, THORNTON, C & LIPSCOMB, C 2001, '*Articulated Concrete Block Stability Testing*', Journal of the American Water Resources Association, vol. 1.
2. AMTI Force and Motion 2009, *MC3-SSUDW Underwater force sensor*, AMTI Force and Motion, viewed 3rd August 2016, <http://amti.biz/select%20product%20PDFs/Force%20sensors/MC3-SSUDW.pdf>.
3. Australian Maritime College 2016, *Circulating Water Channel Information*, Australian

Maritime College, viewed 9th March 2016, <https://www.amc.edu.au/maritime-engineering/circulating-water-channel>.

4. FIGLIOLA, RS & BEASLEY, D 2015, *Theory and design for mechanical measurements*, John Wiley & Sons.
5. FRANCIS, J 2013, '*Experimental Study of Hydrodynamic Forces Acting on a Concrete Mattress in Current*', Australian Maritime College.
6. GODBOLD, J, SACKMANN, N & CHENG, L 2014, '*Stability Design for Concrete Mattresses*', in The Twenty-fourth International Ocean and Polar Engineering Conference.
7. GRIGGS, R 2014, '*3D CFD Investigation of hydrodynamic forces on subsea articulated concrete mattresses*', Edith Cowan University.
8. LAGASSE, PF 2007, *Countermeasures to protect bridge piers from scour*, vol. 593, Transportation Research Board.
9. MCLAREN, R 2015, '*Investigation of Hydrodynamic Forces on Articulated Concrete Block Mattresses in Fluid Flow from Various Horizontal Directions*', Australian Maritime College.
10. MELVILLE, B 2006, '*Bridge abutment scour: estimation and protection*', Australian Journal of Water Resources, vol. 10, no. 1, pp. 81-92.
11. VERITAS, DN 1988, *On-Bottom Stability Design of Submarine Pipelines*, Veritas, Det Norske.
12. VERITAS, DN 2007, *On-bottom stability design of submarine pipelines*, Veritas, Det Norske.
13. VERITAS, DN 2010, *Environmental conditions and environmental loads*, Veritas, Det Norske.
14. YOUNG, DM & TESTIK, FY 2009, '*Onshore scour characteristics around submerged vertical and semicircular breakwaters*', Coastal Engineering, vol. 56, no. 8, pp. 868-875.

